

Subextensive Entropies and Open Order in Perovskite Oxynitrides

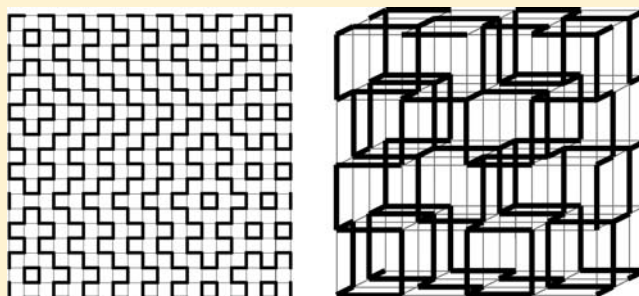
Philip J. Camp,^{*,†} Amparo Fuertes,[‡] and J. Paul Attfield^{*,†,§}

[†]School of Chemistry, The University of Edinburgh, West Mains Road, Edinburgh EH9 3JJ, United Kingdom

[‡]Institut de Ciència de Materials de Barcelona (CSIC), Campus UAB, 08193 Bellaterra, Spain

[§]Centre for Science at Extreme Conditions, The University of Edinburgh, Mayfield Road, Edinburgh EH9 3JZ, United Kingdom

ABSTRACT: Unusual subextensive configurational entropies that vary with particle size and tend to zero per atom in macroscopic samples are predicted for $\text{AMO}_{3-z}\text{N}_z$ oxynitrides with perovskite type crystal structures. These materials are crystallographically disordered on the atomic scale, but local anion order produces chains of M–N–M bonds that undergo a 90° turn at each M cation, giving rise to subextensive entropies in materials such as SrTaO_2N , LaNbON_2 , and $\text{EuWO}_{1.5}\text{N}_{1.5}$. A general Pauling ice-rules formula is used to calculate the extensive molar entropies for other cases such as $\text{SrMoO}_{2.5}\text{N}_{0.5}$ and BaTaO_2N . The subextensive oxynitrides are usefully classified as showing an “open order”, related to the correlated order of displacements in ferroelectric perovskites such as BaTiO_3 . This raises the possibility that further open-ordered oxynitride or molecular structures may be accessible, and other states such as spins and charges may also show novel open orders.



related to the correlated order of displacements in ferroelectric perovskites such as BaTiO_3 . This raises the possibility that further open-ordered oxynitride or molecular structures may be accessible, and other states such as spins and charges may also show novel open orders.

INTRODUCTION

Configurational entropies provide useful information about atomic correlations and local order, and they may sometimes be predicted from simple statistical models as in Pauling’s famous calculation of the residual entropy of ice.¹ Configurational entropies for crystalline materials containing atomic disorder are normally extensive, being proportional to the number of atoms. A recent study has revealed that $\text{AMO}_{3-z}\text{N}_z$ perovskite oxynitrides contain chains of M–N–M bonds that undergo a 90° turn at each M cation, for which Pauling ice-rules predict zero configurational entropy despite the apparent structural disorder.² This unusual observation prompted the full entropy analysis presented here.

The ideal AMX_3 perovskite structure consists of small M cations at the vertices of a simple cubic cell bridged by anions X at the centers of all edges and a large A cation at the cell center. The lattice contains an infinite cubic network of vertex sharing MX_6 octahedra. Most perovskites are based on a single anion such as oxide or fluoride, but transition-metal oxynitride perovskites $\text{AMO}_{3-z}\text{N}_z$ have been of recent interest for their optical and electronic properties.^{3,4} Although full long-range anion order is not observed in these materials, a recent analysis of SrMO_2N (M = Nb, Ta) showed that well-defined *cis*- MO_4N_2 octahedra are present, resulting in disordered zigzag MN chains within two-dimensional perovskite layers.² Perovskite-like layers of disordered zigzag chains are also expected in the K_2NiF_4 -type oxynitrides $\text{Sr}_2\text{NbO}_3\text{N}$,⁵ $\text{Sr}_2\text{TaO}_3\text{N}$,⁶ and $\text{Ba}_2\text{TaO}_3\text{N}$.⁷ The constraint that the chains must turn by 90° at each M site (with the same condition on zigzag MO chains in $\text{AMO}_{3-z}\text{N}_z$ when $z > 1.5$, e.g. LaNbON_2)⁸ is not observed in other materials or in magnetic analogues of crystalline atomic materials such as spin ices. Here we explore the configurational

entropies of the principal $\text{AMO}_{3-z}\text{N}_z$ structural models that arise from this unusual structural constraint. Some structures have the unusual property of being subextensive, where the entropy per atom tends to zero in macroscopic samples, while others have extensive entropies that are estimated by extending Pauling’s ice model. We also report a new classification of structures based on their sets of long- and short-range correlation vectors, from which the unusual “open ordered” nature of the subextensive oxynitride structures is apparent.

RESULTS

i. Pauling Entropies of Perovskite Oxynitrides.

Configurational entropies of $\text{AMO}_{3-z}\text{N}_z$ perovskites are estimated by extending Pauling’s ice model to a general lattice of N M cations, each connected to n other M cations by either M–N–M or M–O–M bridges, so there are in total $nN/2$ bridges. The number of M–N–M bridges emanating from each M cation is denoted by x ($x = 2z$ for $\text{AMO}_{3-z}\text{N}_z$ perovskites) so that the total number of M–N–M bridges is $xN/2$ and the fractions of M–N–M and M–O–M bridges are $f = x/n$ and $(1 - f)$, respectively. In the absence of local bonding constraints, the number of ways of arranging the M–N–M bridges is

$$W = \frac{(nN/2)!}{(fnN/2)![(1-f)nN/2]!}$$

A mean-field approximation for the fraction of allowable configurations is p^N , where

Received: January 26, 2012

Published: March 23, 2012

$$p = wf^x(1-f)^{n-x} = wf^{fn}(1-f)^{(1-f)^n}$$

is the probability of an M ion having its bonding constraints satisfied, and w is the number of ways of orienting M-N-M bridges to the M cation's n neighbors. Using Stirling's approximation ($\ln N! \approx N \ln N - N$), the entropy is

$$S = k_B \ln(Wp^N) \approx Nk_B \ln[wf^{fn/2}(1-f)^{(1-f)n/2}]$$

As a check, identifying M-N-M and M-O-M bridges with donor and acceptor hydrogen bonds in ice, there are $w = 6$ local configurations per molecule, $n = 4$ hydrogen bonds for each O atom, and a fraction $f = 1/2$ of donor hydrogen bonds; this recovers Pauling's famous estimate $S = R \ln(3/2)$ for hexagonal water ice,¹ which is accurate to within 1% of values from more detailed calculations and experimental measurements.⁹

The two anion distributions found in AMO₂N perovskites (and AMON₂ analogues) are represented by SrTaO₂N and BaTaO₂N. In SrTaO₂N types (including materials such as SrNbO₂N, EuTaO₂N, EuNbO₂N, and CaTaO₂N),¹⁰ the zigzag M-N-M chains are confined to two-dimensional planes. Assuming that each possible structure is degenerate, ordered structures such as that in Figure 1a are possible but statistically

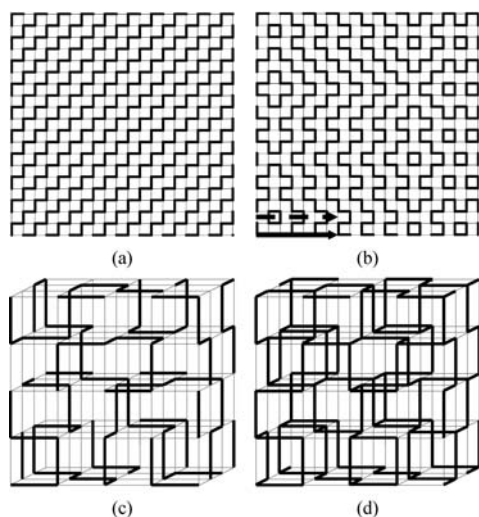


Figure 1. Models for the *cis*-anion chains in oxynitride perovskites, where heavy/light lines correspond to M-N-M/M-O-M connections: (a) long-range ordered and (b) disordered (but open-ordered) configurations of *cis*-MN chains confined to two-dimensional planes within AMO₂N materials such as SrTaO₂N. The solid and dashed arrows on part b, respectively, represent long-range ($\xi \rightarrow \infty$) and short-range ($\xi = 0$) anion ordering correlations parallel to the horizontal axis. This structure has subextensive configurational entropy. (c) Three-dimensionally disordered *cis*-MN chains in BaTaO₂N; the fraction of M-N-M connections is 1/3, and the structure has extensive configurational entropy. (d) Cross-linked chains in the AMO_{1.5}N_{1.5} perovskites where three mutually *cis* M-N-M bridges meet at each M cation and define three-dimensional zigzag patterns on a cubic lattice. The entropy is subextensive, and the structure has three-dimensional open order.

unlikely (and have not been observed experimentally), and it is overwhelmingly likely that any randomly generated structure will show disorder, such as that shown in Figure 1b. This corresponds to a *cis* variant of the square-ice lattice,¹¹ where M-N/M-O bonds map on to short/long O-H bonds in ice, and only structures in which the two short O-H bonds are adjacent (*cis*) to one another are allowed.¹² This variant of the

well-known ice model¹³ is little explored, although other variants have been devised for ferroelectric ordering in KH₂PO₄¹⁴ and for antiferroelectric orders.¹⁵ The AMO₂N model for SrTaO₂N types has $n = 4$ bridges per M atom and a fraction of M-N-M connections $f = 1/2$, but the *cis* constraint restricts the number of allowed local configurations to $w = 4$ (the number of edges of a square) and gives $S = 0$, as noted previously.² Such structures that give $S = 0$ in the Pauling approximation have subextensive entropies, as described in section ii.

BaTaO₂N does not show deviations from cubic symmetry that would reflect confinement of the N atoms to two-dimensional planes,¹⁶ so the zigzag TaN chains are assumed to propagate in all three dimensions (Figure 1c). Two *cis* M-N-M bridges link each metal ion on a cubic lattice so $n = 6$ and $f = 1/3$. The number of ways for an M cation to be linked by two M-N-M bridges in a *cis* conformation is $w = 12$ (the number of edges of an octahedron). These parameters give an extensive (nonzero) configurational entropy of $S = 2R \ln(4/3) \approx 0.58R$ per mole (where $R = 8.314 \text{ J K}^{-1} \text{ mol}^{-1}$ is the molar gas constant). Hence, the molar configurational entropies of AMO₂N materials are predicted to vary from zero in the two-dimensional SrTaO₂N limit, to 0.58R in the disordered cubic BaTaO₂N structure. Intermediate situations might be realized by quenching SrTaO₂N from high temperatures where some propagation of TaN chains between planes was observed,² so that the order is not purely two-dimensional.

In the proposed model for AMO_{1.5}N_{1.5} perovskites such as magnetoresistive EuWO_{1.5}N_{1.5},¹⁷ and the pigment (La_{0.5}Ca_{0.5})-TaO_{1.5}N_{1.5},¹⁸ each M cation is bonded to three nitrogen atoms in a mutual *cis* conformation—also known as the *fac* (facial) configuration of an octahedron—so that the M-N-M bridges define three-dimensional zigzag patterns on a cubic lattice (Figure 1d). Each M cation has $n = 6$ neighbors, the fraction of M-N-M bridges is $f = 1/2$, the number of ways for M to be linked by $x = 3$ M-N-M *cis* bridges in a *fac* conformation is $w = 8$ (the number of faces of an octahedron), and so the Pauling estimate of the entropy is $S = 0$.

In oxynitride perovskites with $z = 0.5$, such as SrMoO_{2.5}N_{0.5},¹⁹ each M cation has one N neighbor. If these are distributed equally in all three dimensions, then there are $w = 6$ local configurations (the number of vertices of an octahedron) for the connection of an M cation to its $n = 6$ neighbors; the fraction of M-N-M bridges is $f = 1/6$ and the molar configurational entropy is $S = (R/2) \ln(3125/1296) \approx 0.44R$. If the N atoms were confined to planes as in SrMO₂N (M = Nb, Ta), then the parameters would change to $n = w = 4$ and $f = 1/4$, and the molar configurational entropy would be $S = (R/2) \ln(27/16) \approx 0.26R$. Confinement of N atoms to one of the three cubic axes gives $n = w = 2$ and $f = 1/2$, giving another case where $S = 0$. Detailed neutron studies of anion distributions in AMO_{2.5}N_{0.5} perovskites have not been reported, so there is no experimental evidence for two- or one-dimensional confinements of the N atoms.

The expected evolution of configurational entropy with composition in AMO_{3-z}N_z perovskites is summarized in Figure 2. The striking feature is the suppression of a measurable entropy near $z = 1.5$ due to the formation of subextensive states, and at $z = 1$ and $z = 2$ when the minority anions are confined to planes, as observed in SrTaO₂N, LaNbON₂, etc. This is contrary to normal expectations for a disordered system such as AMO_{3-z}N_z, where the maximum extensive entropy is expected to occur at the $z = 1.5$ midpoint. The EuWO_{3-z}N_z

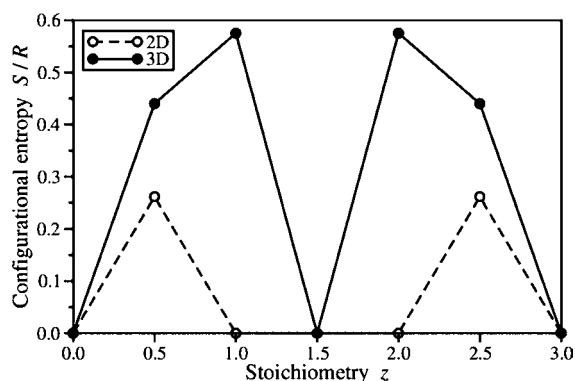


Figure 2. Plot of predicted molar configurational entropy against composition for $\text{AMO}_{3-z}\text{N}_z$ perovskites. Data are shown per mole of M cations, with the minority anions (N for $z < 1.5$, O for $z > 1.5$) constrained in *cis* conformations to two dimensions (2D—open symbols, dashed lines) or to three dimensions (3D—filled symbols, solid lines).

series, which has a wide composition range $1.5 < z < 2.2$ reflecting variable cation oxidation states, is thus predicted to show two configurational entropy minima at $z = 1.5$ and 2.0 .¹⁷

ii. Subextensive Perovskite Oxynitrides. Several of the above models are predicted to have zero configurational entropy, but it is unclear in the Pauling approach whether a small finite entropy would be obtained from a more detailed treatment. An exact result is obtained by noting that the bonding constraints for structures such as those in Figure 1b and d generate strictly alternating M-N-M and M-O-M bridges along the rows of the lattice. Hence, there are only two possible sequences for each row. In the SrTaO_2N model where the MN chains are confined to layers as in Figure 1b, the number of configurations of an $L \times L \times L$ lattice of L layers each containing $2L$ rows is $W = 2^{2L^2}$. For $N = L^3$ M cations, the configurational entropy is $S = k_B \ln W = 2N^{2/3}k_B \ln 2$, where k_B is Boltzmann's constant. This type of entropy is "subextensive", as the exponent of the number of atoms N is less than one, so that the entropy per atom becomes vanishingly small for large N , in asymptotic agreement with the Pauling result. Particles containing N formula units have a configurational entropy of $S = (2R \ln 2)/N^{1/3}$ per mole of SrTaO_2N , showing that the entropy of such a subextensive material is strongly dependent on the particle size. A single crystal containing one mole ($N = N_A$, the Avogadro number) of SrTaO_2N has $S \approx 10^{-7}R$, which would not be measurable, but a powder of 40 nm nanoparticles, each containing $N \approx 10^6$ formula units, has a significant configurational entropy of $S \approx 0.1R$ per mole of SrTaO_2N .

The configurational entropy of the $\text{AMO}_{1.5}\text{N}_{1.5}$ perovskite model is similarly subextensive. Here the M-N-M bridges define three-dimensional zigzag patterns on a cubic lattice, and these bonding constraints imply alternating M-N-M and M-O-M bridges along any row of the cubic lattice. Following the previous argument, the exact number of configurations is $W = 2^{3L^2}$ for $3L^2$ rows in an $L \times L \times L$ cubic lattice and so $S = 3N^{2/3}k_B \ln 2$, which is again subextensive. Hence, the molar configurational entropy of $\text{EuWO}_{1.5}\text{N}_{1.5}$, like that of SrTaO_2N , is predicted to be strongly dependent on the particle size. Confinement of N atoms to one of the three cubic axes in $\text{AMO}_{2.5}\text{N}_{0.5}$ perovskites would also create subextensive states, although no experimental evidence for this partial anion order has been reported.

iii. Open Order. The unusual nature of the anion ordering in oxynitride perovskites is illustrated by the subextensive configurational entropies predicted above. Subextensive phases form an intermediate category of translationally ordered matter, between perfectly ordered crystals such as β' -CuZn (β' -brass) and quasicrystals, which ideally have zero configurational entropy, and disordered crystals, such as the random alloy β -CuZn (β -brass), which have extensive configurational entropies. The configurational entropies of subextensive materials are practically zero in the macroscopic limit, but they appear crystallographically disordered. Disordered packings of well-ordered chains or layers (e.g., random stacking of close-packed slabs is observed in many intercalation compounds such as the battery cathode material LiCoO_2) also have subextensive entropies, but the unusual nature of the oxynitrides is apparent from the crystal directions in which atoms are correlated. The model for oxynitride planes in SrTaO_2N (Figure 1b) shows that M-N-M and M-O-M bridges alternate perfectly along vectors in the vertical and horizontal directions but order over only a few unit cell lengths in other in-plane directions defined by sums or differences of the vertical and horizontal vectors. This is expressed below using correlation lengths ξ , where the probability that atoms at two sites separated by distance d satisfies a particular ordering rule is proportional to $\exp(-d/\xi)$.

Perfect crystals of linear dimension La (where a is the cubic lattice spacing) have long-range order with $\xi \gg La$ (written here as $\xi \rightarrow \infty$) in all lattice directions, whereas disordered crystals have zero or short-range correlations $\xi \ll La$ (written as $\xi = 0$) in all directions. The correlation lengths in all possible $[UVW]$ directions (for vector $U\mathbf{a} + V\mathbf{b} + W\mathbf{c}$, where \mathbf{a} , \mathbf{b} , and \mathbf{c} are the unit cell vectors and U , V , and W are integers) fall into $\xi \rightarrow \infty$ and $\xi = 0$ sets. For perfectly ordered crystals such as β' -CuZn, all $[UVW]$ vectors are in the $\xi \rightarrow \infty$ set and the $\xi = 0$ set is empty. In mathematical terminology, these sets are "closed" under addition or subtraction operations, as all sums or differences of $[UVW]$ vectors fall into the same $\xi \rightarrow \infty$ set as the $[UVW]$ vectors themselves, and the null $\xi = 0$ set is also closed under these operations. The two sets are also closed under addition or subtraction operations for disordered structures such as that of β -CuZn, as all $[UVW]$ vectors fall in the $\xi = 0$ set.

A full classification of the subextensive states for two-state (Ising) orderings (e.g., of O/N at anion sites in the oxynitride models in section ii) along the crystal axes is shown in Table 1. Perfectly ordered alternating chains parallel to the axes can be formed in up to $c = 3$ directions. Atomic planes defined by two of these chain-ordered axes may be fully ordered, so the maximum possible number of ordered planes p is cC_2 . For $c = 2$ axes, only the plane defined by these axes may be ordered; for example, only the xy plane for chains parallel to the x and y axes, but for $c = 3$ directions, up to three planes (xy , xz , and yz) may be ordered. The $p = 3$ condition implies the full long-range order of a perfect crystal.

Structures with subextensive entropy have $\xi \rightarrow \infty$ in some directions within the crystal and $\xi = 0$ in others, and one of the two sets of $[UVW]$ vectors is not closed (hence "open") under addition or subtraction operations. Disordered stackings of well ordered chains or planes have an open $\xi = 0$ set. For instance, when $c = 2$ and $p = 1$, long-range ordered layers stacked randomly in the z direction have all $[UV0]$ vectors in the $\xi \rightarrow \infty$ set, so this is closed, but the $\xi = 0$ set is open, e.g. because the subtraction of $[101]$ from $[201]$ gives $[100]$ in the $\xi \rightarrow \infty$ set. However, the subextensive oxynitrides fall into a separate

Table 1. Types of Translationally-Ordered Structures, Classified by the Number of Orthogonal Axes along Which Long-Range Ordered ($\xi \rightarrow \infty$) Chains Are Oriented (c), and the Number of Long-Range Ordered Planes Containing These Chains (p)^a

c	p	$S/k_B \ln 2$	ordered ($\xi \rightarrow \infty$) set closure	disordered ($\xi = 0$) set closure	atomic and displacive examples
0	0	N	closed (null)	closed	<i>β-CuZn</i>
1	0	$N^{2/3}$	closed	open	<i>VO(H₂AsO₄)₂</i>
2	0	$2N^{2/3}$	open	closed	<i>SrTaO₂N</i>
2	1	$N^{1/3}$	closed	open	<i>LiCoO₂</i>
3	0	$3N^{2/3}$	open	closed	<i>EuWO_{1.5}N_{1.5}</i> , <i>C-BaTiO₃</i>
3	1	$N^{2/3} + N^{1/3}$	open	closed	<i>T-BaTiO₃</i>
3	2	$2N^{1/3}$	open	closed	<i>O-BaTiO₃</i>
3	3	0	closed	closed (null)	<i>β'-CuZn</i> , <i>R-BaTiO₃</i>

^aThe configurational entropy in each case is shown for Ising-like systems of N atoms, each having two possible states (e.g. oxide/nitride site occupation). The open or closed nature of the sets of $[UVW]$ lattice vectors with correlation length $\xi \rightarrow \infty$ or $\xi = 0$ is indicated (see text). The $c = p = 0$ (top row) and $c = p = 3$ (bottom row) cases correspond to normal disordered and ordered crystals with extensive and zero configurational entropies, respectively. The intermediate cases have subextensive entropies, and the unusual oxynitrides also have open sets of $\xi \rightarrow \infty$ vectors (“open order”). Examples of atomic and displacive orderings are shown in roman and italic text, respectively.

class where the $\xi \rightarrow \infty$ set is open; for example, for xy -plane oxynitride layers such as those in Figure 1b with $c = 2$ and $p = 0$, there are $\xi \rightarrow \infty$ vectors parallel to $[100]$ and $[010]$ but not to $[110]$ or $[\bar{1}10]$. $\xi = 0$ vectors also run parallel to $[100]$ and $[010]$, as shown in Figure 1b, and in all other directions, so the $\xi = 0$ set contains all $[UVW]$ vectors and is thus closed.

The above set closure conditions are usefully shortened to “closed/open order/disorder”, where “closed/open” refers to whether or not a set of $[UVW]$ vectors is closed under addition or subtraction operations, and “order/disorder” refers to the $\xi \rightarrow \infty/\xi = 0$ sets. Hence, perfectly ordered crystals and random alloys show both closed order and closed disorder. Subextensive states have open order or disorder; those based on random stackings of well-ordered chains or layers have open disorder, but the oxynitride structures are distinctive from other types of translationally ordered structure by having open order.

Although subextensive atomic orders are rare in simple solids, analogous displacive orders are better-established and provide useful comparisons. For example, the formation of VO^{2+} vanadyl groups within chains of corner-linked VO_6 octahedra gives rise to randomly oriented $\text{O}-\text{V}-\text{O}-\text{V}-\text{O}-\text{V}-\text{O}$ chains parallel to a single axis in $\text{VO}(\text{H}_2\text{AsO}_4)_2$,²⁰ corresponding to the $c = 1$ case in Table 1. The open-ordered $c = 3$ $\text{AMO}_{1.5}\text{N}_{1.5}$ structure is directly related to ferroelectric perovskites such as BaTiO_3 and LiNbO_3 . In $\text{AMO}_{1.5}\text{N}_{1.5}$, each M cation is connected to three mutually *cis* N atoms, and three mutually *cis* O atoms, while local displacements of Ti toward an octahedral face in BaTiO_3 result in three mutually *cis* short Ti–O bonds and three mutually *cis* long Ti–O bonds. However, the long-range orderings of the constituent units along rows in the two cases are opposite to one another (Figure 3). In the oxynitrides, the long-range anion-ordered structure N–M–O–M–N–M–O–M–N creates antiferroelectrically

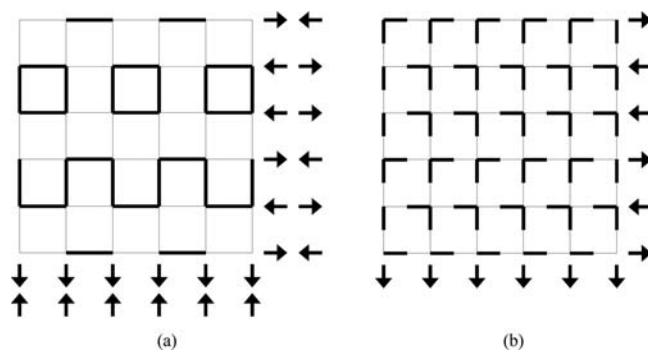


Figure 3. Illustrations of the structural analogy between correlated anions in $\text{AMO}_{1.5}\text{N}_{1.5}$ and atomic displacements in ferroelectric perovskites: (a) an oxynitride perovskite plane showing M–N–M/M–O–M connections as heavy/light lines; (b) an analogous ferroelectric plane in BaTiO_3 , obtained by replacing N–M–O connections from left to right and top to bottom in part a with O–Ti–O connections in part b. Short Ti–O/long Ti–O bonds are shown as heavy/light lines. Both structures have subextensive configurational entropies. The correlated displacive order in part b gives rise to a net electrical polarization for each plane as displayed by the arrows, whereas in part a the chains are antiferroelectric but the relative order of dipoles is analogous. The drawn configurations have long-range order between the vertical chains but zero or short-range correlations between successive horizontal chains. Part b illustrates the order in the intermediate orthorhombic and tetragonal phases of BaTiO_3 , where chain polarizations are long-range ordered parallel to two and one of the three perovskite axes, respectively.

aligned dipoles $\rightarrow\leftarrow\rightarrow\leftarrow$ ($\rightarrow = \text{N–M–O}$), whereas the $\text{O}-\text{Ti}-\text{O}-\text{Ti}-\text{O}-\text{Ti}-\text{O}-\text{Ti}-\text{O}$ structure in BaTiO_3 constitutes ferroelectric ordering of the dipoles $\rightarrow\rightarrow\rightarrow\rightarrow$ ($\rightarrow = \text{O}-\text{Ti}-\text{O}$).

BaTiO_3 undergoes a series of transitions between phases of different symmetry on heating: rhombohedral (R) \rightarrow orthorhombic (O) \rightarrow tetragonal (T) \rightarrow cubic (C). The first three structures are ferroelectric while the cubic phase is paraelectric, and they have been described using an order–disorder model of dipole chains.²¹ In the limit that the dipole correlations within chains parallel to the three cubic axes ($c = 3$ in Table 1) are of long-range, as proposed in a recent computational study,²² the sequence of phase transitions corresponds to decreasing the number of ordered planes: $p = 3 \rightarrow 2 \rightarrow 1 \rightarrow 0$ on heating. The $p < 3$ phases have subextensive configurational entropies, and the measured BaTiO_3 transition entropies are found to be consistently small ($0.02R$ – $0.06R$);²³ the recent study suggested that changes in the phonon spectrum are the main contribution.²² This relationship raises the question of whether ordered phases of $\text{AMO}_{1.5}\text{N}_{1.5}$ analogous to the three ferroelectric phases of BaTiO_3 can be formed (see Figure 3). Achieving long-range order of anions is a future challenge for perovskite oxynitride chemistry—careful high-temperature annealing studies will be needed to investigate this possibility.

DISCUSSION

Translationally ordered matter falls into three classes on the basis of the exponent s for the variation of configurational entropy with number of atoms, $S \sim N^s$. Classical ordered and disordered crystals respectively have $s = 0$ and 1, and the intermediate class of subextensive matter described above has $0 < s < 1$. Subextensive phases represent the most highly correlated states of matter that are possible without adopting a

full long-range ordered crystal structure. Within the sub-extensive category, open atomic order is unusual, as it requires atoms to participate in intersecting well-ordered chains or layers without generating long-range order in intermediate directions. The two-dimensional AMO_2N (Figure 1b) and three-dimensional $\text{AMO}_{1.5}\text{N}_{1.5}$ (Figure 1d) structures are canonical examples of atomically open-ordered arrangements. In the latter model, each M atom lies at the intersection of three perfectly ordered N-M-O-M-N-M-O-M-N chains parallel to the cubic axes, but no long-range order arises in any other direction. Open-ordered structures arise spontaneously in these oxynitrides due to the strong preference for *cis*-N-M-N bonding. We note that molecular chemistry can be used to synthesize larger units that possess the same geometric characteristics, such as *cis* isomers of square planar MX_2Y_2 complexes, or *fac*- MX_3Y_3 octahedra, and open-ordered packings may result when either X...Y or X...X and Y...Y intermolecular interactions dominate.

Direct magnetic analogues of the atomic and displacive open orders on simple cubic lattices are not known and present a challenge for the design of new magnetic systems. Open spin orders on frustrated lattices have been reported; for example, antiferromagnetic Ising models (AFMIMs) on a honeycomb lattice²⁴ and on an elastic triangular lattice²⁵ have subextensive entropies which scale as $N^{1/2}$ per layer (equivalent to the $N^{2/3}$ scaling for the SrTaO_2N -type structure in Results section ii, where stacks of layers were considered).

Throughout this work it has been assumed that the energies of all configurations are equal, so configurational contributions to the free energy are insufficient to drive an ordering transition on cooling. A recent study of the elastic AFMIM identified an “order by disorder” mechanism by which the degeneracy of the ground states may be lifted, leading to a stabilization of partially disordered zigzag arrangements of ferromagnetically aligned spins stabilized by the phonon contribution to the free energy.²⁴ In the unfrustrated perovskites displaying open anion or displacive orders, Coulombic forces are likely to drive the system to a full long-range closed order, as observed in the low-temperature rhombohedral form of BaTiO_3 .

Many other atomic variables such as ionic charges in mixed-valent materials and orbital states (and their consequent Jahn–Teller displacements) can show order/disorder phenomena on periodic lattices. Open charge orders could be of interest in the context of charge fluctuation mechanisms for superconductivity in doped copper oxides. Arrangements of larger objects such as colloidal particles in optical crystals²⁶ can also show classical ordered and disordered states, and again it is intriguing to consider whether open orders could be achieved on the mesoscale and what the resulting properties might be.

CONCLUSIONS

$\text{AMO}_{3-2}\text{N}_z$ perovskite oxynitride structures provide interesting examples of ice-type disorder on square or cubic lattices. The local *cis*-coordination rule gives rise to predicted subextensive entropies in materials such as SrTaO_2N , LaNbON_2 , and $\text{EuWO}_{1.5}\text{N}_{1.5}$. The subextensive structures are usefully classified as showing an “open order”, related to the correlated local order of displacements in ferroelectric perovskites such as BaTiO_3 .

AUTHOR INFORMATION

Corresponding Author

philip.camp@ed.ac.uk; j.p.attfield@ed.ac.uk

Notes

The authors declare no competing financial interest.

ACKNOWLEDGMENTS

This work was supported by EPSRC, EaStCHEM, and the Leverhulme Trust, U.K., and the Ministerio de Economía y Competitividad (Grants MAT2011-24757 and SAB2011-0047), Spain.

REFERENCES

- (1) Pauling, L. *J. Am. Chem. Soc.* **1935**, *57*, 2680–2684.
- (2) Yang, M.; Oró-Solé, J.; Rodgers, J. A.; Jorge, A. B.; Fuertes, A.; Attfield, J. P. *Nature Chem.* **2011**, *3*, 47–52.
- (3) Ebbinghaus, S. G.; Abicht, H.-P.; Dronskowski, R.; Müller, T.; Reller, A.; Weidenkaff, A. *Prog. Solid State Chem.* **2009**, *37*, 173–205.
- (4) Fuertes, A. *Dalton Trans.* **2010**, *39*, S942–S948.
- (5) Tobías, G.; Beltrán-Porter, D.; Lebedev, O. I.; Van Tendeloo, G.; Oró-Solé, J.; Rodríguez-Carvajal, J.; Fuertes, A. *Inorg. Chem.* **2004**, *43*, 8010–8017.
- (6) Diot, N.; Marchand, R.; Haines, J.; Léger, J. M.; Macaudière, P.; Hull, S. *J. Solid State Chem.* **1999**, *146*, 390–393.
- (7) Clarke, S. J.; Hardstone, K. A.; Michie, C. W.; Rosseinsky, M. J. *Chem. Mater.* **2002**, *14*, 2664–2669.
- (8) Logvinovich, D.; Ebbinghaus, S. G.; Reller, A.; Marozau, I.; Ferri, D.; Anke Weidenkaff, A. *Z. Anorg. Allg. Chem.* **2010**, *636*, 905–912.
- (9) Nagle, J. F. *J. Math. Phys.* **1966**, *7*, 1484–1491.
- (10) Gunther, E.; Hagenmayer, R.; Jansen, M. *Z. Anorg. Allg. Chem.* **2000**, *626*, 1519–1525.
- (11) Lieb, E. H. *Phys. Rev.* **1967**, *162*, 162–172.
- (12) Pete, G. *Ann. Probab.* **2008**, *36*, 1711–1747.
- (13) Baxter, R. J. *Exactly Solved Models in Statistical Mechanics*; Academic Press: 1982.
- (14) Slater, J. C. *J. Chem. Phys.* **1941**, *9*, 16–33.
- (15) Rys, F. *Helv. Phys. Acta* **1963**, *36*, 537–559.
- (16) Page, K.; Stoltzfus, M. W.; Kim, Y.-I.; Proffen, T.; Woodward, P. M.; Cheetham, A. K.; Seshadri, R. *Chem. Mater.* **2007**, *19*, 4037–4042.
- (17) Yang, M.; Oró-Solé, J.; Kusmartseva, A.; Fuertes, A.; Attfield, J. P. *J. Am. Chem. Soc.* **2010**, *132*, 4822–4829.
- (18) Jansen, M.; Letschert, L. P. *Nature* **2000**, *404*, 980–982.
- (19) Fawcett, I. D.; Ramanujachary, K. V.; Greenblatt, M. *Mater. Res. Bull.* **1997**, *32*, 1565–1570.
- (20) Aranda, M. A. G.; Attfield, J. P.; Bruque, S.; Martínez-Lara, M. *Inorg. Chem.* **1992**, *31*, 1045–1049.
- (21) Comes, R.; Lambert, M.; Guinier, A. *Solid State Commun.* **1968**, *6*, 715–719.
- (22) Zhang, Q.; Cagin, T.; Goddard, W. A., III. *Proc. Natl. Acad. Sci.* **2006**, *103*, 14695–14700.
- (23) Chaves, A. S.; Barreto, F. C. S.; Nogueira, R. A.; Zeks, B. *Phys. Rev. B* **1976**, *13*, 207–212.
- (24) Andrews, S.; De Sterck, H.; Inglis, S.; Melko, R. G. *Phys. Rev. E* **2009**, *79*, 041127.
- (25) Shokef, Y.; Souslov, A.; Lubensky, T. C. *Proc. Natl. Acad. Sci. (USA)* **2011**, *108*, 11804–11809.
- (26) Han, Y.; Shokef, Y.; Alsayed, A. M.; Yunker, P.; Lubensky, T. C.; Yodh, A. G. *Nature* **2008**, *456*, 898–902.